Journal of Environmental Management 209 (2018) 105–111

Contents lists available at ScienceDirect

Journal of Environmental Management

journal homepage: www.elsevier.com/locate/jenvman

Research article

Novel biochar-impregnated calcium alginate beads with improved water holding and nutrient retention properties

Bing Wang [a, b, d], Bin Gao [b, *], Andrew R. Zimmerman [c], Yulin Zheng [b], Honghong Lyu [b]

[a] State Key Laboratory of Environmental Geochemistry, Institute of Geochemistry, Chinese Academy of Sciences, Guiyang, 550081, China
[b] Department of Agricultural and Biological Engineering, University of Florida, Gainesville, FL, 32611, USA
[c] Department of Geological Sciences, University of Florida, Gainesville, FL, 32611, USA
[d] Puding Karst Ecosystem Research Station, State Key Laboratory of Environmental Geochemistry, Institute of Geochemistry, Chinese Academy of Sciences, Puding, 562100, China

ARTICLE INFO

Article history:
Received 27 July 2017
Received in revised form
12 December 2017
Accepted 17 December 2017
Available online 4 January 2018

Keywords:
Biochar
Ball milling
Calcium alginate beads
Controlled release
Water holding capacity
Soil amendment

ABSTRACT

Drought conditions and nutrients loss have serious impacts on soil quality as well as crop yields in agroecosystems. New techniques are needed to carry out effective soil water and nutrient conservation and fertilizer application tools. Here, calcium alginate (CA) beads impregnated with ball-milled biochar (BMB) were investigated as a new type of water/nutrients retention agent. Both CA and Ca-alginate/ball milled biochar composite (CA-BMB) beads showed high kinetic swelling ratios in KNO_3 solution and low kinetic swelling ratios in water, indicating that CA-BMB beads have the potential to retain mineral nitrogen and nutrients by ion exchange. Pseudo-second-order kinetic model well-described the swelling kinetics of both beads in KNO_3 solution. Over a range of temperatures, the characteristics of dehydration suggested that impregnation with BMB improved the water holding capacity and postponed the dehydration time of Ca-alginate. The cumulative swelling and release characteristics of water, K^+, and NO_3^- indicated that CA-BMB beads have great potential as a soil amendment to improve its nutrient retention and water holding capacity.

1. Introduction

Chemical fertilizers are widely applied in most modern mainstream agricultural settings. For example, fertilizer addition is estimated to be responsible for about 40–60% of the global grain yield (Roberts, 2009). Nitrogen (N), phosphorus (P) and potassium (K) are the most common nutrients limiting plant growth (Dai et al., 2013; Zörb et al., 2014). While fertilizer application rates are high, nutrient use efficiency is very low. For example, it is estimated that only about 33 percent of the applied N is utilized by various crops and the remaining nutrients are lost via leaching, run-off, gaseous emission and fixation by soil microbes (Baligar et al., 2001). The low use efficiency of fertilizer is a problem that has plagued the world's agriculture, both reducing food supply and farmers' profits (Shaviv and Mikkelsen, 1993b).

The main pathways of soil N and P loss are surface runoff, leaching, soil erosion, ammonia volatilization, nitrification, and denitrification. Because fertilizer-supplied N and P are mainly in the form of NO_3^- and PO_4^-, respectively, they are poorly sorbed by the mainly negatively charged soil particles and easily lost following rainfall or irrigation. Runoff and leaching of N and P are also a non-point source of pollution that can lead to aquatic eutrophication (Huang et al., 2017; Wang et al., 2014). Potassium (K), another key nutrient, plays a particularly crucial role in a number of physiological processes vital to growth, yield, quality, and stress resistance of all crops (Zörb et al., 2014). In natural systems, soil K becomes available to plants mainly by water-solubilization of minerals (Jaiswal et al., 2016). However, exchangeable K is often sorbed by soil colloids which are then carried off and lost from the soil.

Besides nutrients, water is of course essential for plant growth and it is the biggest limiting factor in the world's ability to feed a growing population. Therefore, it would be of great benefit to agricultural and society to find a practical soil conditioner that can minimize losses of water and nutrient elements from the soil. Such a conditioner would sorb and then slowly release water and nutrients so that they can be taken up and used by plants efficiently (Shaviv and Mikkelsen, 1993a).

* Corresponding author.
E-mail address: bg55@ufl.edu (B. Gao).

https://doi.org/10.1016/j.jenvman.2017.12.041
0301-4797/

In recent years, biochar began to attract attention as a soil amendment with the potential to increase plant productivity while sequestering atmospheric CO_2 (Lehmann, 2007; Lehmann and Joseph, 2009). Biochar is made by high-temperature pyrolysis of crop biomass such as crop stalks, livestock and poultry manure and other agricultural wastes, and then applied to farmland soil using appropriate methods and standards (Lehmann and Joseph, 2015). Previous studies have found that biochar might increase soil water-holding capacity and have the ability to sorb soil macronutrients such as N and P (Basso et al., 2013; DeLuca et al., 2009; Karhu et al., 2011; Lehmann et al., 2003; Yu et al., 2013). When applied to the soil, biochar can also be a source of soil nutrients and can increase the activity of soil microorganisms (Biederman and Harpole, 2013; Prendergast-Miller et al., 2014). After a great deal of recent research, studies still disagree as to whether the productivity enhancement effect of biochar is primarily through stimulation of the native microbial community, the release of new nutrients, or through its regulation of native nutrients (Biederman and Harpole, 2013).

The ability of biochar to improve the retention of some soil nutrients can be attributed to its large specific surface area, porosity and many negative surface functional groups, all of which produce its enhanced soil cation exchange capacity (Mukherjee et al., 2011). Biochar addition may also improve nutrient retention by increasing soil pH and soil organic matter mineralization rate (Laird et al., 2010; Liang et al., 2006; Méndez et al., 2012). While studies have shown that biochar can hold nutrient elements and reduce their release (Mukherjee and Zimmerman, 2013)., because of its negative charge, the attraction of N (and P) to biochar is relatively weak. Compared with other sorbents, freshly made biochar usually has low anion adsorption capacity (Yao et al., 2012). Ball milling has been shown to significantly increase the surface area, porosity, and surface functional group contents of biochar (Lyu et al., 2018a, 2018b). Ball-milled biochars are likely to have improved water holding and nutrient retention characteristics.

An issue with ball-milled biochar, however, is that its small particle size may make it difficult to apply to soils in an agricultural setting and more easily lost from soil via runoff and infiltration. Previous studies have shown that transport of biochar increased with decreasing particle size (Wang et al., 2013; Zhang et al., 2010) and a significant fraction of biochar particles move to lower soil layers in saturated sandy soil, especially biochar particles of nanometer scale (Wang et al., 2013). Particles of biochars in soils, being relatively lighter than other soil solids, are also prone to preferential erosion and off-site transport in surface runoff. The consequences of the movement of biochar colloids is the off-site migration of sorbed pesticides and other contaminants which leads to a potential risk to ground and surface water (Chen et al., 2017; Kookana, 2010). Thus, this work also explores the stabilization of ball-milled biochar (BMB) by its immobilization onto gel beads.

Alginate beads have been widely used for the delivery of bioactive materials and for entrapment of contaminants or nutrients in the environmental settings including agricultural soils (Escudero et al., 2009; Luo and Zhang, 2009; Pasparakis and Bouropoulos, 2006; Thakur et al., 2016; Wang et al., 2017). Alginate can form a gel and separate from water in a process called ionotropic gelation (Patil et al., 2012). Much research has been carried out to study the factors influencing the gelation process (Bajpai and Sharma, 2004; Rassis et al., 2002; Roy et al., 2009; Smrdel et al., 2008; Sriamornsak, 1999) and has been reviewed (Bajpai and Sharma, 2004). However, few studies have examined potential uses of these gels in agriculture (Karadağ et al., 2000), and none in combination with biochar. Thus, it was hypothesize that addition of BMB to Ca-alginate will improve its ability to retain water and nutrients. This work was aimed at determining the suitability of calcium alginate/ball-milled biochar composites as a soil amendment to improve water and nutrient management and enhance agricultural sustainability.

2. Materials and methods

2.1. Chemicals and reagents

High viscosity sodium alginate from *macrosytica pyrifera* (MP Biomedicals, Inc. Co., USA), calcium chloride ($CaCl_2$) and potassium nitrate (KNO_3) were purchased from Fisher Scientific. All the chemicals and reagents were of reagent grade and used without any further purification.

2.2. Preparation of BMB

Bamboo biomass was oven dried (80 °C) and then converted into biochar through slow pyrolysis using a furnace (Olympic 1823HE) in an N_2 environment at peak temperatures of 450 °C. The biochar was mechanically activated in a planetary ball mill (Across International, PQ-N_2) under air atmosphere at room temperature in lidded 500 mL capacity agate milling jars. The milling ball-to-biochar weight ratio was 10:1 and the rotational speed of the main disk was 300 rpm. Each biochar was milled for a total of 12 h, reversing milling direction every 3 h.

2.3. Preparation of beads

To achieve a uniform dispersion, sodium alginate (1% w/v) mixed with BMB was sonicated using a Model B3510-MT Ultrasonic Cleaner (Branson Ultrasonics Co., USA) which has a nominal frequency of 40 kHz, for 2 h at 25 °C. While stirring at 400 rpm the BMB dispersion was thoroughly mixed with a suspension of sodium alginate (1% w/v) at the mass ratio of 0.25 (BMB/alginate). While stirring, 100 mL of this colloidal solution was added dropwise into 500 mL of 0.1 M $CaCl_2$ solution and then were left overnight to stabilize. The beads were then rinsed several times with deionized water to remove residual BMB particles and non-cross-linked Ca ions from the surface of the beads. Finally, the beads were dried in an oven at 50 °C for 24 h. Pure Ca-alginate beads were prepared separately for use as controls.

2.4. Material characterization

A number of methods were used to characterize the BMB, CA and CA-BMB. Thermogravimetric analysis of the samples was performed in a stream of N_2 (50 mL min^{-1}) at a heating rate of 10 °C min^{-1} from 30 °C to 700 °C using a Mettler TGA analyzer (Columbus, OH). The structure and surface morphology of bamboo biochar and ball-milled biochar, CA and CA-BMB (pristine and loaded with KNO_3) were examined using scanning electron microscopy/energy-dispersive X-ray spectroscopy (SEM/EDX) using a JSM-6460LV Scanning Microscope (JEOL, Tokyo, Japan). The size of alginate and Ca-alginate-BMB gel particles were measured using calipers.

2.5. Swelling capacity, kinetics and dehydration

The ability of the dried CA and CA-BMB beads to sorb water, i.e. the swelling capacity, was evaluated using gravimetric analysis. Swelling capacity was quantified as the swelling ratio (D_s):

$$Ds = \frac{Wt - W0}{W0} \quad (1)$$

where W_0 and W_t are the weights of the samples in the dry and saturated states, respectively.

To measure swelling kinetics, 10 mg of sample was placed in distilled water (pH 7.0) in 100 mL beakers and sampled at predetermined time intervals (0, 0.083, 0.25, 0.5, 1, 2, 4, 8, 16, 24 h). The swollen beads were gently pressed between two filter paper sheets to remove excess water and finally weighed on a digital balance.

The dehydration of CA and CA-BMB beads was monitored as weight loss over time, measured using the TGA at 20, 30, and 50 °C to simulate soil drying at different temperatures. Each TGA run was carried out using 10–20 mg of swollen sample, following the swelling kinetic experiments.

2.6. Nutrient loading and release

Loading of K^+ and $NO_3^-$was measured as weight gain after equilibrating preweighed dry beads in an aqueous solution of KNO_3 (1% w/v) for 48 h. The weight percent loading was calculated as:

$$\%\text{Loading} = \frac{m1 - m0}{m0} \times 100\% \quad (2)$$

where m_1 and m_0 are the weights of KNO_3-loaded and pristine dry beads, respectively.

To study the release of K^+ and NO_3^-, 10 mg samples of nutrient-loaded beads were placed in distilled water (20 mL) under unstirred condition. At scheduled time intervals (0.5, 1, 2, 3, 4, 5, 6, 12, 24, 48, 72, 96 h), 10 mL solution aliquots were removed and filtered through a 0.45 μm membrane filter (Whatman). An equivalent volume (10 mL) of distilled water was added to the solution with the beads to keep return the volume to 20 mL. The released amount of K^+ and NO_3^- at each time interval was determined by measurement of filtrate concentrations of K^+ by inductively coupled plasma optical emission spectrometer (ICP-OES, Optima 2100 DV, Perkin Elmer, USA), and NO_3^- by UV–Vis spectrophotometer at 665 nm wavelength (GENESYS 10S, Thermo Fisher Scientific) in the filtrate.

2.7. Data treatment

All the experiments and analytical measurements were conducted in triplicate. Mean values are shown in the plotted data with the standard deviation represented as the error bars. Paired sample t-test analysis was conducted using SPSS19.0 (SPSS Inc.) to evaluate whether differences between means were significant ($p < 0.01$).

To evaluate and compare the uptake and release characteristics of the materials, pseudo-first-order, pseudo-second-order, Elovich and Ritchie models were used to simulate the experimental kinetic data:

$$R_t = R_C\left(1 - e^{-k_1 t}\right), \quad \text{Pseudo} - \text{first} - \text{order} \quad (3)$$

$$R_t = \frac{k_2 R_c^2 t}{1 + k_2 R_c t}, \quad \text{Pseudo} - \text{second} - \text{order} \quad (4)$$

$$R_t = \frac{1}{\beta}\ln(\alpha\beta t + 1), \quad \text{Elovich} \quad (5)$$

$$R_t = R_C - \left(R_C^{1-n}\frac{k_n}{1-n}t\right)^{\frac{1}{1-n}}, \quad \text{Ritchie} \quad (6)$$

where R_t (%) and R_c (%) are the cumulative ratios of sorbed or released components at time t and at equilibrium, respectively; k_1 (h^{-1}), k_2 (% h^{-1}), and k_n (h^{-1}) are the first-order, second-order, and Ritchie nth-order sorption or release rate constants; α (% h^{-1}) is the initial release rate, and β ($\%^{-1}$) is the sorption or release rate constant.

3. Results and discussion

3.1. Characterization of materials

The specific surface area of pristine bamboo biochar before and after ball milling was 18.2 and 298.6 $m^2\ g^{-1}$, respectively. Scanning electron micrographs (SEMs) show the unmilled and ball-milled biochar (BMB) to be about 5 and 1 μm particle size, respectively (Fig. 1 a and b), accounting for the 16-fold increase in surface area. The alginate beads were nearly spherical, initially and as composites with the BMB (Fig. 1 c and d) with mean diameters of approximately 2.2 mm. but shrinking to 0.5 mm after drying.

Thermo-gravimetric analysis (TGA) shows BMB to have had negligible weight losses below a temperature of about 300 °C (Fig. 2), similar to biochars of previous studies (Sun et al., 2014). The CA decomposition process begins around 200 °C due to the removal of surface bound water and continues to 257 °C. Finally, mass loss due to volatile emission occurred at 600 °C with a total remaining mass of 23% (carbonaceous residues). For CA-BMB, the pattern was similar except that higher temperature decomposition was delayed indicating that thermal stability was improved after incorporation of BMB with CA.

3.2. Beads swelling kinetics

An understanding of swelling kinetics is useful for predicting the uptake of water and nutrients. The swelling ratio of CA and CA-BMB in H_2O was only 1.5 and 1.3, respectively. In 1% KNO_3, however, the swelling ratio of the CA and the CA-BMB beads were 144.7 and 147.9 respectively, or about 100 times greater (Fig. 3). The majority of swelling of the test beads in KNO_3 solution occurred within 10 min. Both swelling curves were best modeled using a pseudo-second-order kinetic model, similar to other CA bead studies (Lagoa and Rodrigues, 2009). However, the swelling kinetics of CA and CA-BMB in water (not shown) did not display the same kinetic behavior. These results suggested that the presence of nutrients (e.g., 1% KNO_3) promoted water absorbance by the dried CA and CA-BMB beads. Fig. 3 shows that this kinetics obeys Fick's second law of diffusion until the swelling reaches equilibrium. The Fick diffusion law considers that the diffusion coefficient of the diffuser and the thickness of the diffusion film are constants throughout the diffusion process. In this work, however, the size of the beads was changing during the swelling, suggesting it had little effect on the diffusion process. Zactiti and Kieckbusch also found that the influence of swelling on effective diffusivity is small, suggesting that alginate films have a potential use for release of active substances (Zactiti and Kieckbusch, 2009).

3.3. Dehydration curves

Dehydration times for CA beads and CA-BMB ranged from about 40 min at 50 °C to about 225 min at 20 °C (Fig. 4). In general, CA beads lost water faster than CA-BMB beads suggesting that BMB impregnation within CA increased its water retention capacity. Several studies have found that biochar addition to soil improved its water holding capacity (Abel et al., 2013; Beck et al., 2011) and this was attributed to the large pore volume, complex porosity structure and high specific surface area of biochar (Carrier et al., 2012; Mohamed et al., 2016). These properties of biochar are increased further by ball milling (Peterson et al., 2012; Shan et al., 2016). It has also been found that the presence of polar oxygen-containing groups raises the hydrophilicity of biochar and aids the formation of hydrogen bonds (Pastor-Villegas et al., 2010). Apparently, the ability of BMB to hold water was retained even when encapsulated within CA.

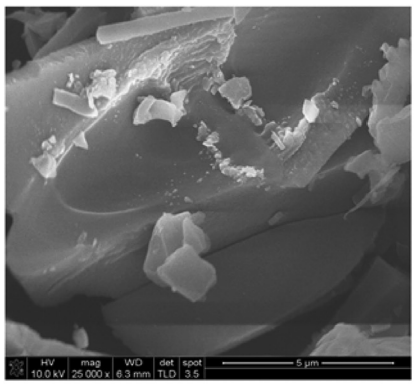

(a) Bamboo biochar

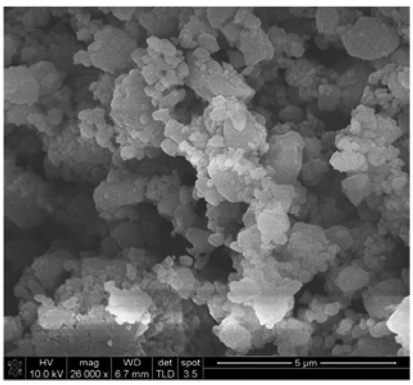

(b) Ball milled bamboo biochar

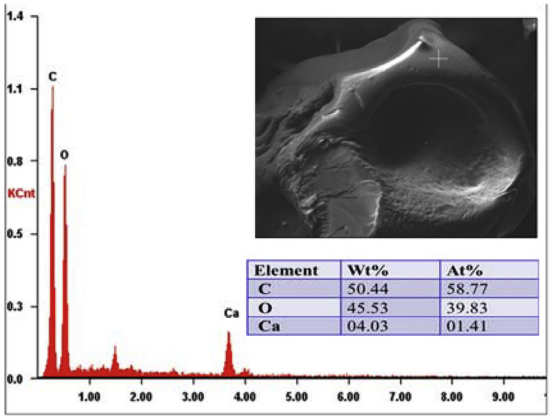

(c) CA beads unloaded

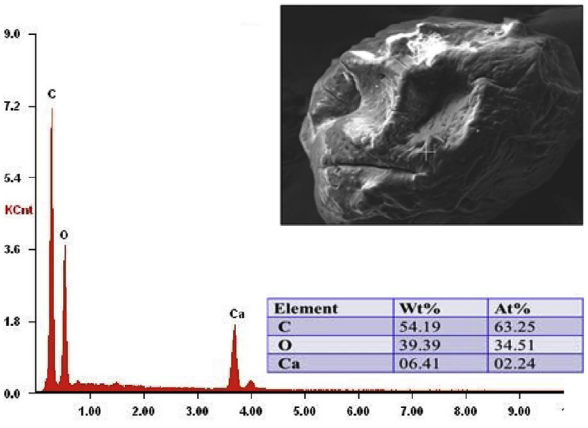

(d) CA-BMB unloaded

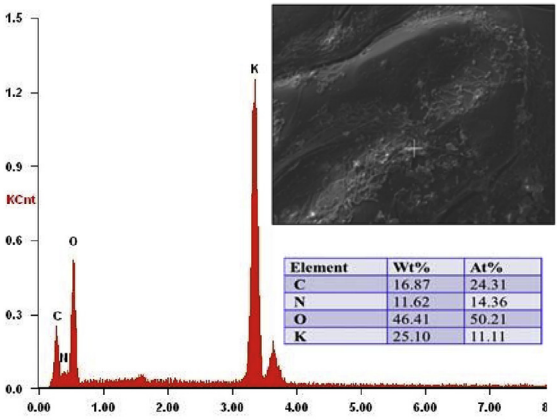

(e) Ca-alginate-loaded

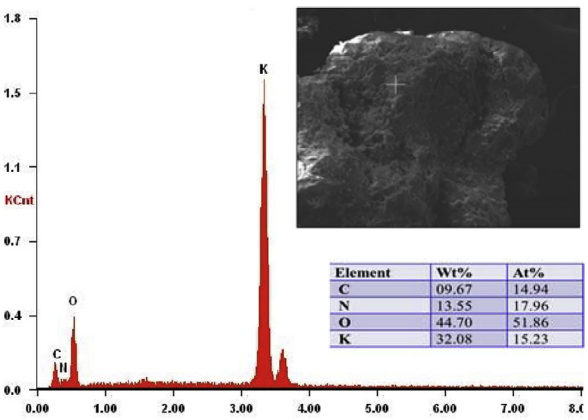

(f) Ca-alginate-BMB loaded

Fig. 1. Scanning electron micrographs and EDX elemental compositions of (a) Bamboo biochar; (b) Ball milled biochar,; (c) pristine CA beads, (d) pristine CA-BMB beads, (e) K^+ and NO_3^--loaded CA beads, and (f) K^+ and NO_3^--loaded CA-BMB beads.

3.4. Evaluation nutrient holding capacity

As calculated from equation (2), the percent loading of KNO_3 on CA and CA-BMB was 48.1% and 64.1%, respectively. Thus, addition of BMB significantly improved the nutrient holding capacity of CA ($p < 0.01$). SEM images of the K^+ and NO_3^--loaded CA beads (Fig. 1e) and loaded CA-BMB beads (Fig. 1f) show their surfaces to have gained a roughened appearance, perhaps indicative of precipitates, likely potassium nitrate, on their surfaces. EDX elemental distributions show elemental concentrations of N and K reaching about 18 and 15%, respectively, in the loaded CA-BMB beads. Notably, the N/K ratios in the loaded CA and CA-BMB beads were about the same (1.2).

When the KNO_3-loaded beads were placed into distilled water, about 30% of the K^+ and about 5–10% of the NO_3^- was released in the first half hour (Fig. 5). It may be that the potassium nitrate crystals attached to the surface of the beads quickly dissolved into the water during this period. With additional time, K and N ions inside the beads were gradually released into solution by ion exchange. After 20 h, the cumulative releases of K^+ and NO_3^- reached a steady state.

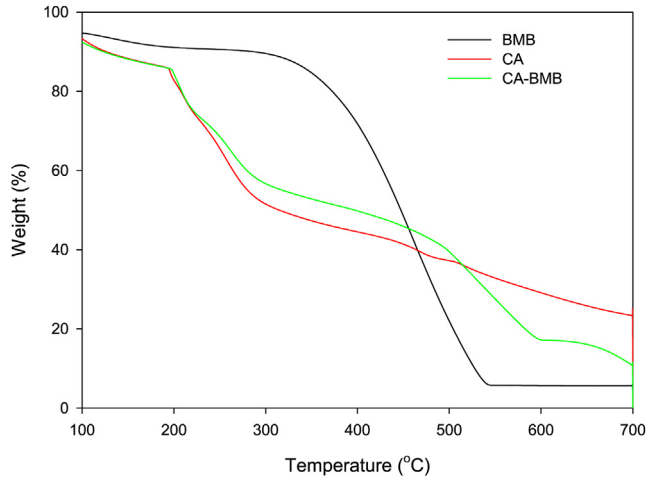

Fig. 2. Thermogravimetric curves of Ca-alginate (CA) beads, ball-milled biochar (BMB), and Ca-alginate-ball milled biochar composite (CA-BMB).

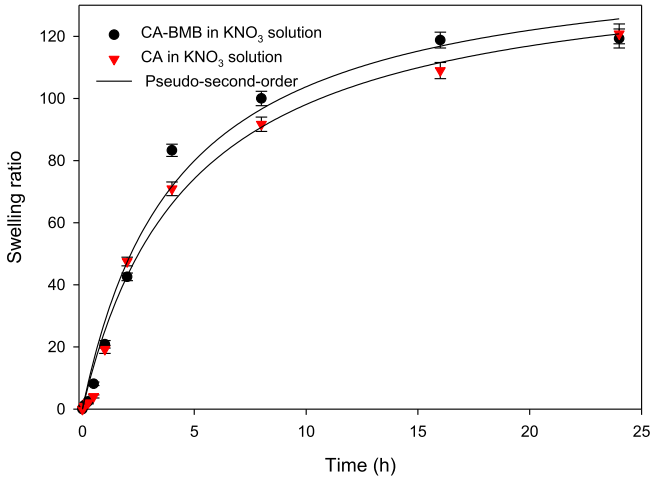

Fig. 3. CA and CA-BMB swelling ratio in 1% (w/v) KNO_3 solution as a function of time.

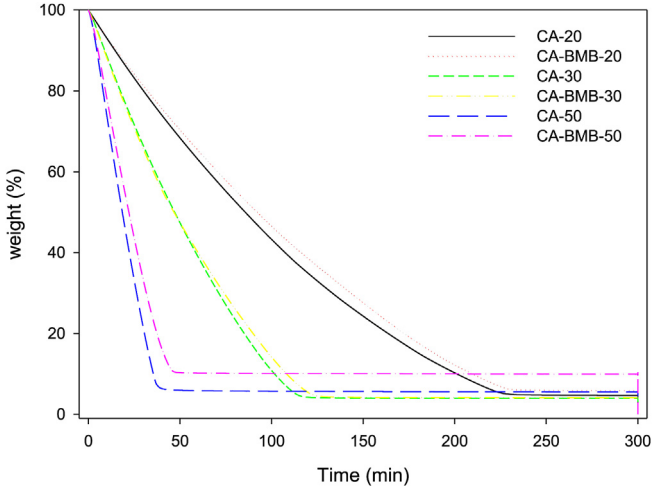

Fig. 4. Dehydration curves of CA and CA-BMB beads at different temperatures (20, 30, and 50 °C indicated as numbers after sample names in legend).

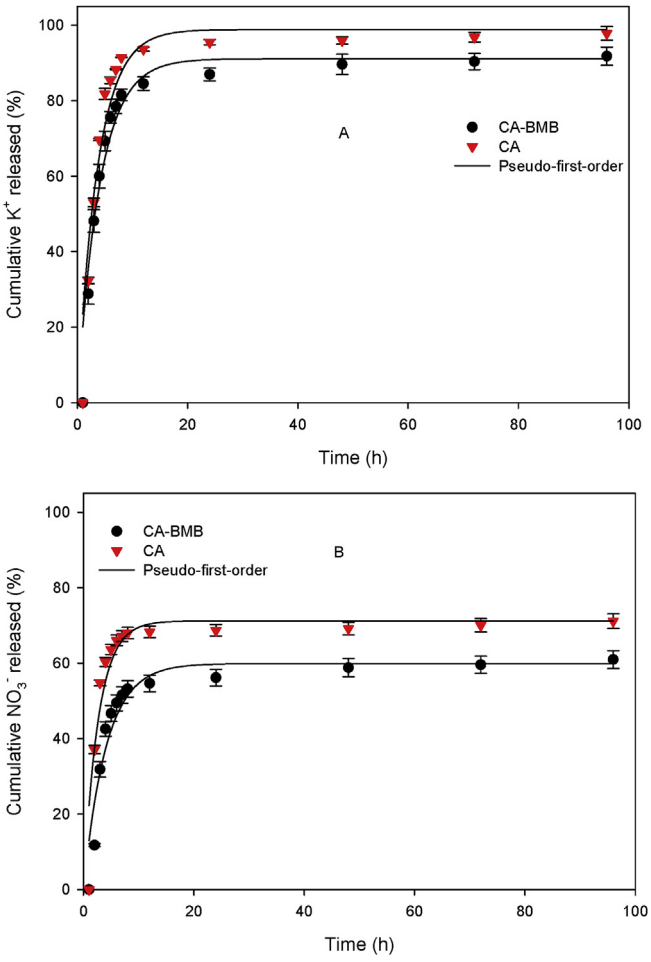

Fig. 5. The cumulative amounts of K^+ (A) and NO_3^- (B) released from Ca-alginate (CA) and Ca-alginate/ball milled biochar composite (CA-BMB) beads over time.

More than 80% and 90% of K^+ were released from CA and CA-BMB, respectively, in about 24 h (Fig. 5), and equilibrium was reached in 96 h. According to the fitting results (Table 1), the pseudo-first-order model was the best model describing the kinetic experimental data. This kinetics modelling suggests that release of K^+ from CA and CA-BMB was mainly controlled by the diffusive transport of the K^+ within the pore network of the beads (Apel and Torma, 1993). Compared with CA beads, the CA-BMB beads released less K^+ released, indicating that impregnation of CA with BMP increases the retention of K^+.

The pattern of cumulative release of NO_3^- from CA and CA-BMB show characteristics similar to K^+ release. However, the portion of NO_3^- released from both CA and CA-BMB was lower than that of K^+ (Fig. 5b). Compared to the release of K^+, the release process of NO_3^- from CA and CA-BMB was found to be relatively fast with more than 50% and 70% of NO_3^- released from CA and CA-BMB, respectively, in about 20 h before reaching equilibrium. The lower cumulative release of nitrate can be attributed to the relatively low anion exchange capacity of ball milled biochar. However, there might have been some N loss as gas. Another reason might be due to the release kinetics of NO_3^- from CA and CA-BMB was mainly controlled by the diffusive transport of the NO_3^- within the pore network of the beads. Compared with CA beads, the CA-BMB beads show less NO_3^- released which indicated that the CA-BMB could retain more NO_3^- after impregnating with BMB. The probable reason for this was because biochars could adsorb nitrate by bridge bonding using the charge of electrostatically attracted (Mukherjee et al., 2011).

Table 1
Summary of best-fit parameters of various kinetic models for K^+ and NO_3^- release from CA and CA-BMB beads.

	Adsorbent	Model	Parameter 1	Parameter 2	R^2
K^+	CA	Pseudo-first order	$k_1 = 0.271$	Rc = 98.9	0.924
		Pseudo-second order	$k_2 = 0.0034$	Rc = 108.1	0.839
		Elovich	$\alpha = 161.30$	$\beta = 0.0596$	0.638
		Ritchie	$k_n = 0.000004$	Rc = 91.2	0.893
	CA-BMB	Pseudo-first order	$k_1 = 0.248$	Rc = 91.1	0.940
		Pseudo-second order	$k_2 = 0.003$	Rc = 100	0.875
		Elovich	$\alpha = 221.8$	$\beta = 0.0822$	0.614
		Ritchie	$k_n = 0.000003$	Rc = 91.3	0.940
NO_3^-	CA	Pseudo-first order	$k_1 = 0.374$	Rc = 71.2	0.874
		Pseudo-second order	$k_2 = 0.007$	Rc = 77.4	0.768
		Elovich	$\alpha = 373.37$	$\beta = 0.0994$	0.510
		Ritchie	$k_n = 0.000006$	Rc = 71.3	0.873
	CA-BMB	Pseudo-first order	$k_1 = 0.244$	Rc = 59.9	0.911
		Pseudo-second order	$k_2 = 0.0048$	Rc = 66.1	0.846
		Elovich	$\alpha = 66.147$	$\beta = 0.0909$	0.683
		Ritchie	$k_n = 0.0000028$	Rc = 71.3	0.774

4. Conclusions

The impregnation impregnated CA beads with ball-milled biochar resulted in a novel composite with enhanced water and nutrient holding capacities, and good controlled-release properties. Thus, CA-BMB beads, when added to soil, may be especially useful for improving water retention in arid and semi-arid soils.

Acknowledgement

This work was financially supported by the National Program on Key Basic Research Project (2016YFC0502602), the National Science Foundation of China (Grant No. U1612441), the Key Agriculture R & D Program of Guizhou Province (NZ [2013]3012), the International Scientific and Technological Cooperation Project of Guizhou Province (G[2012]7050), the "Dawn of West China" Talent Training Program of the Chinese Academy of Sciences (grant number [2012] 179) and the Opening Fund of State Key Laboratory of Environmental Geochemistry (SKLEG2014912, SKLEG2016910).

References

Abel, S., Peters, A., Trinks, S., Schonsky, H., Facklam, M., Wessolek, G., 2013. Impact of biochar and hydrochar addition on water retention and water repellency of sandy soil. Geoderma 202–203, 183–191.
Apel, M., Torma, A., 1993. Determination of kinetics and diffusion coefficients of metal sorption on ca-alginate beads. Can. J. Chem. Eng. 71, 652–656.
Bajpai, S.K., Sharma, S., 2004. Investigation of swelling/degradation behaviour of alginate beads crosslinked with Ca^{2+} and Ba^{2+} ions. React. Funct. Polym. 59, 129–140.
Baligar, V., Fageria, N., He, Z., 2001. Nutrient use efficiency in plants. Commun. Soil Sci. Plant Anal. 32, 921–950.
Basso, A.S., Miguez, F.E., Laird, D.A., Horton, R., Westgate, M., 2013. Assessing potential of biochar for increasing water-holding capacity of sandy soils. Gcb Bioenergy 5, 132–143.
Beck, D.A., Johnson, G.R., Spolek, G.A., 2011. Amending greenroof soil with biochar to affect runoff water quantity and quality. Environ. Pollut. 159, 2111–2118.
Biederman, L.A., Harpole, W.S., 2013. Biochar and its effects on plant productivity and nutrient cycling: a meta-analysis. Gcb Bioenergy 5, 202–214.
Carrier, M., Hardie, A.G., Uras, Ü., Görgens, J., Knoetze, J., 2012. Production of char from vacuum pyrolysis of South-African sugar cane bagasse and its characterization as activated carbon and biochar. J. Anal. Appl. Pyrol. 96, 24–32.
Chen, M., Wang, D., Yang, F., Xu, X., Xu, N., Cao, X., 2017. Transport and retention of biochar nanoparticles in a paddy soil under environmentally-relevant solution chemistry conditions. Environ. Pollut. 230, 540–549.
Dai, X., Ouyang, Z., Li, Y., Wang, H., 2013. Variation in yield gap induced by nitrogen, phosphorus and potassium fertilizer in north China plain. PloS One 8, e82147.
DeLuca, T.H., MacKenzie, M.D., Gundale, M.J., 2009. Biochar effects on soil nutrient transformations. Biochar Environ. Manage. Sci. Technol. 251–270.
Escudero, C., Fiol, N., Villaescusa, I., Bollinger, J.-C., 2009. Arsenic removal by a waste metal (hydr)oxide entrapped into calcium alginate beads. J. Hazard. Mater. 164, 533–541.
Huang, J., Xu, C.-C., Ridoutt, B.G., Wang, X.-C., Ren, P.-A., 2017. Nitrogen and phosphorus losses and eutrophication potential associated with fertilizer application to cropland in China. J. Clean. Prod. 159, 171–179.
Jaiswal, D.K., Verma, J.P., Prakash, S., Meena, V.S., Meena, R.S., 2016. Potassium as an Important Plant Nutrient in Sustainable Agriculture: a State of the Art, Potassium Solubilizing Microorganisms for Sustainable Agriculture. Springer, pp. 21–29.
Karadağ, E., Saraydin, D., Çaldiran, Y., Güven, O., 2000. Swelling studies of copolymeric acrylamide/crotonic acid hydrogels as carriers for agricultural uses. Polym. Adv. Technol. 11, 59–68.
Karhu, K., Mattila, T., Bergström, I., Regina, K., 2011. Biochar addition to agricultural soil increased CH_4 uptake and water holding capacity – results from a short-term pilot field study. Agric. Ecosyst. Environ. 140, 309–313.
Kookana, R.S., 2010. The role of biochar in modifying the environmental fate, bioavailability, and efficacy of pesticides in soils: a review. Soil Res. 48, 627–637.
Lagoa, R., Rodrigues, J.R., 2009. Kinetic analysis of metal uptake by dry and gel alginate particles. Biochem. Eng. J. 46, 320–326.
Laird, D.A., Fleming, P., Davis, D.D., Horton, R., Wang, B., Karlen, D.L., 2010. Impact of biochar amendments on the quality of a typical Midwestern agricultural soil. Geoderma 158, 443–449.
Lehmann, J., 2007. A handful of carbon. Nature 447, 143–144.
Lehmann, J., Joseph, S., 2009. Biochar for Environmental Management: Science and Technology. Earthscan/James & James.
Lehmann, J., Joseph, S., 2015. Biochar for Environmental Management: Science, Technology and Implementation. Routledge.
Lehmann, J., Pereira da Silva, J., Steiner, C., Nehls, T., Zech, W., Glaser, B., 2003. Nutrient availability and leaching in an archaeological Anthrosol and a Ferralsol of the Central Amazon basin: fertilizer, manure and charcoal amendments. Plant Soil 249, 343–357.
Liang, B., Lehmann, J., Solomon, D., Kinyangi, J., Grossman, J., O'neill, B., Skjemstad, J., Thies, J., Luizao, F., Petersen, J., 2006. Black carbon increases cation exchange capacity in soils. Soil Sci. Soc. Am. J. 70, 1719–1730.
Luo, X., Zhang, L., 2009. High effective adsorption of organic dyes on magnetic cellulose beads entrapping activated carbon. J. Hazard. Mater. 171, 340–347.
Lyu, H., Gao, B., He, F., Zimmerman, A., Ding, C., Huang, H., Tang, J., 2018a. Effects of ball milling on the physicochemical and sorptive properties of biochar: experimental observations and governing mechanisms. Environ. Pollut. 233, 54–63.
Lyu, H., Gao, B., He, F., Zimmerman, A., Ding, C., Huang, H., Tang, J., Crittenden, J., 2018b. Experimental and modeling investigations of ball-milled biochar for the removal of aqueous methylene blue. Chem. Eng. J. 335, 110–119.
Méndez, A., Gómez, A., Paz-Ferreiro, J., Gascó, G., 2012. Effects of sewage sludge biochar on plant metal availability after application to a Mediterranean soil. Chemosphere 89, 1354–1359.
Mohamed, B.A., Ellis, N., Kim, C.S., Bi, X., Emam, A.E.-R., 2016. Engineered biochar from microwave-assisted catalytic pyrolysis of switchgrass for increasing water-holding capacity and fertility of sandy soil. Sci. Total Environ. 566–567, 387–397.
Mukherjee, A., Zimmerman, A.R., 2013. Organic carbon and nutrient release from a range of laboratory-produced biochars and biochar–soil mixtures. Geoderma 193–194, 122–130.
Mukherjee, A., Zimmerman, A.R., Harris, W., 2011. Surface chemistry variations among a series of laboratory-produced biochars. Geoderma 163, 247–255.
Pasparakis, G., Bouropoulos, N., 2006. Swelling studies and in vitro release of verapamil from calcium alginate and calcium alginate–chitosan beads. Int. J. Pharm. 323, 34–42.
Pastor-Villegas, J., Meneses Rodríguez, J.M., Pastor-Valle, J.F., Rouquerol, J., Denoyel, R., García García, M., 2010. Adsorption–desorption of water vapour on chars prepared from commercial wood charcoals, in relation to their chemical composition, surface chemistry and pore structure. J. Anal. Appl. Pyrol. 88, 124–133.
Patil, P., Chavanke, D., Wagh, M., 2012. A review on ionotropic gelation method: novel approach for controlled gastroretentive gelispheres. Int. J. Pharm. Pharm. Sci. 4, 27–32.

Peterson, S.C., Jackson, M.A., Kim, S., Palmquist, D.E., 2012. Increasing biochar surface area: optimization of ball milling parameters. Powder Technol. 228, 115–120.
Prendergast-Miller, M., Duvall, M., Sohi, S., 2014. Biochar–root interactions are mediated by biochar nutrient content and impacts on soil nutrient availability. Eur. J. Soil Sci. 65, 173–185.
Rassis, D.K., Saguy, I.S., Nussinovitch, A., 2002. Collapse, shrinkage and structural changes in dried alginate gels containing fillers. Food Hydrocolloids 16, 139–151.
Roberts, T., 2009. The role of fertilizer in growing the world's food. Better Crop. 93, 12–15.
Roy, A., Bajpai, J., Bajpai, A., 2009. Dynamics of controlled release of chlorpyrifos from swelling and eroding biopolymeric microspheres of calcium alginate and starch. Carbohydr. Polym. 76, 222–231.
Shan, D., Deng, S., Zhao, T., Wang, B., Wang, Y., Huang, J., Yu, G., Winglee, J., Wiesner, M.R., 2016. Preparation of ultrafine magnetic biochar and activated carbon for pharmaceutical adsorption and subsequent degradation by ball milling. J. Hazard. Mater. 305, 156–163.
Shaviv, A., Mikkelsen, R., 1993a. Controlled-release fertilizers to increase efficiency of nutrient use and minimize environmental degradation-A review. Nutrient Cycl. Agroecosyst. 35, 1–12.
Shaviv, A., Mikkelsen, R.L., 1993b. Controlled-release fertilizers to increase efficiency of nutrient use and minimize environmental degradation - a review. Fert. Res. 35, 1–12.
Smrdel, P., Bogataj, M., Mrhar, A., 2008. The influence of selected parameters on the size and shape of alginate beads prepared by ionotropic gelation. Sci. Pharm. 76, 77.
Sriamornsak, P., 1999. Effect of calcium concentration, hardening agent and drying condition on release characteristics of oral proteins from calcium pectinate gel beads. Eur. J. Pharmaceut. Sci. 8, 221–227.
Sun, Y., Gao, B., Yao, Y., Fang, J., Zhang, M., Zhou, Y., Chen, H., Yang, L., 2014. Effects of feedstock type, production method, and pyrolysis temperature on biochar and hydrochar properties. Chem. Eng. J. 240, 574–578.
Thakur, S., Pandey, S., Arotiba, O.A., 2016. Development of a sodium alginate-based organic/inorganic superabsorbent composite hydrogel for adsorption of methylene blue. Carbohydr. Polym. 153, 34–46.
Wang, D., Zhang, W., Hao, X., Zhou, D., 2013. Transport of biochar particles in saturated granular media: effects of pyrolysis temperature and particle size. Environ. Sci. Technol. 47, 821–828.
Wang, J., Wang, D., Zhang, G., Wang, Y., Wang, C., Teng, Y., Christie, P., 2014. Nitrogen and phosphorus leaching losses from intensively managed paddy fields with straw retention. Agric. Water Manage. 141, 66–73.
Wang, S., Vincent, T., Roux, J.-C., Faur, C., Guibal, E., 2017. Pd(II) and Pt(IV) sorption using alginate and algal-based beads. Chem. Eng. J. 313, 567–579.
Yao, Y., Gao, B., Zhang, M., Inyang, M., Zimmerman, A.R., 2012. Effect of biochar amendment on sorption and leaching of nitrate, ammonium, and phosphate in a sandy soil. Chemosphere 89, 1467–1471.
Yu, O.-Y., Raichle, B., Sink, S., 2013. Impact of biochar on the water holding capacity of loamy sand soil. Int. J. Energy Environ. Eng. 4, 44.
Zactiti, E., Kieckbusch, T., 2009. Release of potassium sorbate from active films of sodium alginate crosslinked with calcium chloride. Packag. Technol. Sci. 22, 349.
Zhang, W., Niu, J., Morales, V.L., Chen, X., Hay, A.G., Lehmann, J., Steenhuis, T.S., 2010. Transport and retention of biochar particles in porous media: effect of pH, ionic strength, and particle size. Ecohydrology 3, 497–508.
Zörb, C., Senbayram, M., Peiter, E., 2014. Potassium in agriculture - status and perspectives. J. Plant Physiol. 171, 656–669.